Journal of Fluids and Structures (1999) **13,** 361–379
Article No.: jfls.1999.0208 available online at http://www.idealibrary.com on IDEAL

NEW DESIGN RECOMMENDATIONS FOR FLUIDELASTIC INSTABILITY IN HEAT EXCHANGER TUBE BUNDLES

K. Schröder and H. Gelbe

Institute of Process and Plant Technology, Technical University of Berlin
Berlin, Germany

(Received 28 July 1997 and in revised form 16 October 1998)

Design equations are presented to determine the critical velocities for the occurrence of fluidelastic instability in uniform single-phase cross-flow. These equations are an essential part of a new guideline in the "VDI-Wärmeatlas" for estimating vibration excitation in real tube bundle heat exchangers. Six existing guidelines for fluidelastic instability were tested and compared with about 300 experimental data from 34 papers (eight of them being not yet considered in a guideline before). New equations for the stability factor K as a function of the pitch ratio for different tube configurations were derived with statistical methods by a variation of the reference definitions for the structural parameters and the exponents of either the dimensionless mass and the damping or the mass-damping parameter. The criterion used here was first to be on the safe side with a minimum number, and minimum deviation, of experimental data below the recommended threshold line, and second a minimum r.m.s. error for all data considered. The pitch ratio has the strongest influence for the normal triangular array and the influence becomes less for the rotated as well as for the in-line square configuration. This significant gradation of the stability constants as a function of the pitch ratio and the tube bundle configuration enables a reasonable interpolation for non-standard configurations. The exponent of the dimensionless mass-damping parameter for gas cross-flow depends on the tube configuration and is 0·5 for the 30°- and 45°-configuration, and 0·4 for the 60°- and 90°-configuration. For liquid flow, an average exponent of 0·15 has been observed.

1. INTRODUCTION

There are three types of flow-induced vibration excitation mechanism which can cause vibration in tube bundle heat exchangers, namely turbulent buffeting, periodic shedding (vortex shedding and acoustic resonance), and fluidelastic instability. Fluidelastic instability is the excitation mechanism with the greatest potential for short-term damage to tube bundles.

The guidelines of Païdoussis (1981), Chen (1987) [see also Chen & Jendrzejczyk (1982) and Chen (1984)], Blevins (1984), Weaver & Fitzpatrick (1988) [see also Weaver & Fitzpatrick (1987)], ASME Pressure Vessel Code (1992) and Pettigrew & Taylor (1991) differ in the choice of the various structural parameters as well as in the determination of the instability threshold. For example, Chen (1987) suggested taking all structural parameters in vacuum and determining the critical velocity with the steep increase of the amplitude versus flow velocity or with the change of the response power spectral density to a narrow-band spectrum (mainly for liquid flow). On the other side, Pettigrew & Taylor (1991) recommended taking all parameters in still fluid and identifying the critical velocity with either the

0889–9746/99/040361 + 19 $30.00

steep increase of the amplitude versus flow velocity for a well-defined instability threshold or by an amplitude limit of 250–750 μm. Weaver & Fitzpatrick (1988) took all parameters in still fluid except for the damping, which is to be determined in still air.

The compiled experimental data of these guidelines and newer experimental data were reviewed from the original papers and transformed to the standard definitions presented in this paper. The existing correlations of the experimental data in all mentioned guidelines were compared; the investigation leads to a different approach to analyse fluidelastic instability data in heat exchanger tube bundles.

2. FLUIDELASTIC INSTABILITY EXCITATION MECHANISM

Tube bundles subjected to cross-flow vibrate even at low fluid velocities. These vibrations are caused by turbulence and possibly superimposed vortex excitation. Fluidelastic instability is based on self-excited forces, which are caused by the interaction between tube motion and fluid flow. Usually, at the onset of fluidelastic instability, fluid forces occur which are proportional to tube displacement and influence the stiffness of the system. This so-called "soft" (Andjelić 1988) or "stiffness-controlled" excitation (Chen 1987) leads to a coordinated motion of all tubes (whirling) and is dominant in low-density fluids and staggered tube configurations. It is superimposed by a second kind of fluid forces, proportional to tube vibration velocities, which reduce the damping of the system. This mechanism leads to a sudden rise of the amplitudes and is called "hard" (Andjelić 1988) or "damping-controlled" excitation (Chen 1987) also known as "galloping". It can become dominant in high-density fluids and in-line tube configurations. The phenomena are described by Chen (1987) and Andjelić & Popp (1989).

The critical velocity of whirling is defined at the point of frequency coordination of all tubes (Chen 1987; Leyh 1993). The stability equation for the dimensionless critical gap velocity u_k^* was derived for whirling by Connors (1970):

$$u_k^* = \frac{u_{sk}}{f_1 d_a} = K\sqrt{\Delta}, \tag{1}$$

where u_{sk} is the critical gap velocity, $\Delta = m\Lambda/(\rho d_a^2)$ is the mass-damping parameter, and K the stability constant.

3. DEFINITION OF DIMENSIONLESS AND STUCTURAL PARAMETERS

Uniform definitions of parameters are important for reviewing data from other researchers. Critical velocity, damping value, frequency, mass per unit length are defined differently by different researchers, so that the dimensionless parameters presented cannot be compared. The data of many researchers had to be transformed to the definitions used in this investigation, i.e., all parameters have to be determined in still fluid with the density ρ. The equations used to transform the data are outlined below. When the mass-damping parameters were given in an accurate way, a missing structural parameter could be recalculated from the equation which defines the mass-damping parameter.

3.1. Mass per Unit Length

The mass per unit length is the effective vibrating mass related to the tube length. It consists of the mass of the tube material including the fluid inside the tube per unit length, m_R, and

the hydrodynamic mass, m_h, defined as

$$m_h = c_h \rho \frac{\pi}{4} d_a^2. \tag{2}$$

The hydrodynamic mass coefficient, c_h, depends on the pitch ratio and can be obtained from Chen (1987).

Chen (1987) and other researchers suggested taking the structural parameters in vacuum for all flow regimes, so that the hydrodynamic mass can be neglected. For this investigation the total mass per unit length had to be calculated for those data in liquid flow, where no hydrodynamic mass or total mass was given. The most accurate way to calculate the total mass per unit length for the known frequency, f_f, in still fluid is via

$$m = m_R \left(\frac{f_g}{f_f}\right)^2. \tag{3}$$

Equation (2) was used only when the frequency f_g in still air was missing and could not be calculated.

3.2. Tube Frequency

In tube bundles, many mode shapes may be excited. For all experimental data investigated it was sufficient to know the first mode. It is recommended to use the tube frequency in still fluid with the density ρ. The tube frequency in still air was also compiled in the database. When tube frequencies were not given, they were calculated, wherever possible.

3.3. Damping

The damping of a vibrating system has an important influence on the magnitude of the amplitude and on the critical velocity. Unfortunately, the prediction of the damping value is a great factor of uncertainty. The most accurate damping values are obtained by measurement in the installed tube bundle. Correlations of published damping data show a deviation of a factor 4 (Pettigrew *et al.* 1986a, b).

The damping values used here were determined in still fluid. If damping values in liquid are not available, they were recalculated from the mass-damping parameter or, in one case (Tanaka and Takahara 1981), by using the damping equations derived by Pettigrew *et al.* (1986a, b) to complete the database.

3.4. Critical Velocity

The different methods for determination of the onset of fluidelastic instability is a source of scatter in the experimental data. Hartlen (1974) used the velocity at which a noticeable sound occurs, which was based on the impact of the tubes. This determination of the critical velocity leads to higher values. On the other hand, Soper (1983) defined the onset of fluidelastic instability as the point at which a tangent to the post-critical response intersected the velocity axis. This method gives an accurate determination of the critical velocity for a well-defined threshold. In other cases, the change of the response power spectral density to a narrow-band spectrum defines the beginning of fluidelastic instability. Austermann & Popp (1995) explained that external forces, for example vortex-induced vibration, can reduce the instability point. This reduction will also occur because of turbulence excitation, which is a source of greater scatter in the liquid flow data.

TABLE 1

Summary of references, fluid, structural and tube-bundle data. And 88 stands for Andjelić (1988), Con 80 for Connors (1980) and so on

	ρ (kg/m^3)	d_a (m)	L (m)	τ	f (Hz)	Λ	m (kg/m)	N	Number of data	Remarks
Tube configuration 30°										
And 88	1·2	0·08	0·8	1·25	9·99	0·026–0·158	3·558	1	23	
Con 80	1·2	0·024	0·202	1·323	19	0·0121	0·573	1	1	
God 84	0·03	0·017–0·026		1·31–1·42	34·2–68·7	0·063	0·3–1·122	12–22	13	2, 4
Gog 82	1·2	0·04	0·996	1·25	14	0·02	1·6	1	1	
Gor 76	1000	0·0127–0·0191	0·94	1·33–1·54	30–40	0·063–0·125	0·281–1·187	1	3	
Gro 75	1·2	0·03	0·271	1·1–1·5	28	0·025	0·7	1	5	
Hal 86	1000	0·0191	3·58	1·25	22·9	0·22	1·093	6	1	2
Hal 88	1000	0·0191	3·58	1·42	24	0·22	0·996	6	1	2
Har 74	1·2	0·0127	0·762	1·25–1·56	4·64–10·02	0·061–0·551	0·058–0·091	1	9	
Hei 81	1000	0·019–0·022	0·91	1·33–1·364	–	–	–	1	2	
Jahr 95	1·2	0·025	1	1·28	48–104·86	0·02–0·4	0·333	3	5	
Kas 94	1000	0·012–0·016	0·25–0·5	1·17–1·64	19·2–134·1	0·029–0·169	0·285–1·099	1	15	
Leyh 93	1·2	0·025	3	1·28	63	0·099	0·333	5	1	2
Min 87	1·2/1000	0·012	0·2	1·3	67·2; 65·9	0·011; 0·03	0·942; 0·98	1	2	
Sop 83	1·2	0·025	0·457	1·25–178	34–36·4	0·22–0·3	0·177–0·278	1	4	
Sto 90	992·2–1284	0·025	1·03	1·28	25·76–28·58	0·114–0·642	1·415–1·742	1	18	
Tro 86	1000	0·012	0·55	1·36	26·1–33·4	0·63–0·94	0·239–0·439	1	2	
Wea 84	1000	0·0127	0·316	1·5	14·6–26·4	0·036–0·083	0·275–1·177	1	3	
Yeu 83	1000	0·0127	0·151	1·5	21·2	0·056	0·587	1	1	
Zuk 80	1000	0·016	0·3	1·15–2	–	–	–	1	8	
Tube configuration 45°										
Abd 86	1000	0·025	0·3	1·41	18·6	0·038	1·22	1	1	
Gor 76	1000	0·0127	0·94	1·3	30	0·125	0·281	1	1	
Hal 86	1000	0·0191	3·58	1·25	23·5	0·22	1·038	6	1	2
Hal 88	1000	0·0191	3·58	1·42	24·4	0·22	0·964	6	1	2
Har 74	1·2	0·0127	0·762	1·25–1·56	4·64–10·02	0·061–0·551	0·058–0·091	1	9	
Hei 81	1000	0·019–0·02223	0·91	1·41–1·5	–	–	–	1	2	
Sop 83	1·2	0·025	0·457	1·27–1·78	32·4–33·5	0·22–0·24	0·177	1	4	
Wea 84	1000	0·0127	0·316	1·5	14·6–26·4	0·036–0·083	0·275–1·177	1	3	3

TABLE 1· *Continued*

Tube configuration 60°										
Aust 93	1·2	0·08	0·8	1·375	9·42	0·03–0·216	3·038	1	17	
Con 80	1·2	0·024	0·2017	1·323	19	–	–	1	1	
Gor 76	1000	0·0127–0·0191	0·94	1·33–1·54	30–40	0·063–0·071	0·495–1·16	1	3	
Hal 86	1000	0·0191	3·58	1·25	22·9	0·22	1·093	6	1	2
Hal 88	1000	0·0191	3·58	1·42	24	0·22	0·996	6	1	2
Har 74	1·2	0·0127	0·762	1·25–1·56	4·64–10·02	0·061–0·551	0·058–0·091	1	9	
Hei 81	1000	0·019–0·022	0·91	1·33–1·364	–	–	–	1	2	
Joh 84	1000	0·015875		1·5	44	0·104	0·614	1	1	
Min 87	1·2/1000	0·012	0·2	1·3	65·9–67·2	0·011–0·03	0·942–0·98	1	2	
Sop 83	1·2	0·025	0·457	1·27–1·78	33·3–33·8	0·24–0·25	0·177	1	4	
Wea 78	1·2	0·0254	0·348	1·375	24	0·007–0·148	0·158	1	8	
Wea 81	1·2	0·0254	0·305	1·375	20	0·017–0·04	0·157–1·784	1	8	
Wea 82	1000	0·0254	0·299	1·375	22·5	0·103	1·163	1	1	3
Wea 83	1000	0·0254	0·3	1·375	15·2	0·035	1·167	1	1	3
Wea 84	1000	0·0127	0·316	1·5	14·6–26·4	0·036–0·083	0·275–1·177	1	3	
Yeu 83	1000	0·0127	0·151	1·5	21·2	0·056	0·587	1	1	
Tube configuration 90°										
Aust 93	1·2	0·08	0·8	1·25	9·42	0·03–0·089	3·038	1	7	
Axi 84	1·2/1000	0·01905	1·19	1·44	51–74	0·013–0·084	0·492–0·574	1	2	
Chen 81	1000	0·0159	0·92 (0·26)	1·5	23·9–25·1	0·145–0·402	1·09–1·20	1	5	
Con 78	1·2/1000	0·024	0·202	1·41–2·125	18–30	0·008–0·153	0·587–1·578	1	6	
Gro 75	1·2	0·03	0·271	1·1–1·5	28	0·025	0·7	1	5	
Hal 86	1000	0·0191	3·58	1·25	23·5	0·22	1·038	6	1	2
Hal 88	1000	0·0191	3·58	1·42	24·4	0·22	0·964	6	1	2
Har 74	1·2	0·0127	0·762	1·25–1·56	4·64–10·02	0·061–0·551	0·058–0·091	1	9	
Hei 81	1000	0·02223	0·91	1·41	–	–	–	1	1	
Kas 94	1000	0·01–0·016	0·25–0·5	1·17–1·64	17·6–134	0·029–0·169	0·285–1·098	1	15	
Lub 86	722·5	0·017	0·325	1·55	647	–	–	1	1	
Sop 83	1·2	0·025	0·457	1·27–1·78	32·1–33·3	0·18–0·25	0·177	1	4	
Sto 90	995–1006	0·025	1·03	1·28	28·4–28·6	0·114–0·339	1·417–1·429	1	10	
Tan 81	1·2/1000	0·03	0·3	1·33	7·56–10	0·004–0·089	1·62–3·464	1	5	1
Tro 86	1000	0·012	0·55	1·36	26·1–33·4	0·063–0·094	0·253–0·414	1	2	
Wea 84	1000	0·0127	0·316	1·5	14·6–26·4	0·036–0·083	0·275–1·177	1	3	
Wea 85	1000	0·025	0·3	1·5	16·9	0·037	1·27	1	1	
Zuk 80	1000	0·018–0·024	0·3	1·15–1·61	20–99	–	–	1	3	

(1) Calculation of the viscous damping part· (2) Full scale data· (3) Influenced by resonant vortex excitation. (4) Total damping was calculated.

No attempt to transform the data to a reference definition was made due to lack of information (e.g. no figures containing amplitude versus flow velocity).

It is also important to consider the different definitions of the reference velocity. Most researchers use the pitch velocity,

$$u_\tau = u_\infty \frac{\tau}{\tau - 1}. \tag{4}$$

Weaver & Yeung (1984) take the maximum gap velocity, which is 0·71 lower for rotated square arrays (45°) and 0·87 lower for the 30°-tube array. The definition used in this paper for the dimensionless critical velocity is the maximum gap velocity related to the frequency in still fluid and the tube diameter, as defined in equation (1).

4. COMPILATION OF DATA FROM LITERATURE

The existing guidelines were used as a basis of this investigation. So, the experimental data compiled by Chen (1987), Weaver & Fitzpatrick (1988) and Pettigrew & Taylor (1991) were evaluated. Only the data by Scott (1987), Blevins *et al.* (1981) and Eisinger (1980) could not be taken into account, because the first two papers were not available, and no complete information on the pitch ratio and other important variables was reported in the last paper. In place of that, eight additional publications, with about 110 experimental data, were considered.

All fluid and structural data were converted to a common reference basis as outlined in Section 3. The standard reference basis was the maximum gap velocity and all parameters evaluated in the still fluid with density ρ; but also the use of the pitch velocity and the recommendation of using all data in still gas were tested. Whenever possible, the structural data reported in the original papers were used directly or after transformation into the standard reference basis. Regarding the data for fluidelastic instability in liquids, it was checked whether an influence due to resonance vortex excitation or vortex shedding was present in the experiments.

The experimental results of 34 papers were compiled in a database containing about 300 data points. They are outlined in the standard reference basis in Table 1.

5. EVALUATION AND PARAMETRIC DEPENDENCE

The object of this study was to find a practicable guideline for real heat exchangers, which would describe the lower bound of the relevant experimental data with a minimum r.m.s. error,

$$(\text{r.m.s. error})^2 = \frac{1}{N} \sum_{i=1}^{N} \left[\frac{u_k^*(\text{data}) - u_k^*(\text{predicted})}{u_k^*(\text{data})} \right]^2 \tag{5}$$

for all the data considered. Several modifications of the Connors equation were recommended. A general formulation of fluidelastic instability reads as follows:

$$u_k^* = K \left(\frac{m}{\rho d_a^2} \right)^c \Lambda^d, \tag{6}$$

where the stability constant K is a function of the tube configuration and the pitch ratio. The compiled experimental data were evaluated for different exponents c and d. The dependence of the calculated stability factor K on the pitch ratio τ was established for

different tube configurations· Data for liquid and gas flow were considered separately. The lowest scatter of the experimental data was observed for identical exponents $c = d$, both for liquid and for gas flow· The general formulation of equation (6) simplifies then to

$$u_k^* = K \left(\frac{m\Lambda}{\rho d_a^2} \right)^P \cdot \tag{7}$$

Publications, in which different exponents c and d are proposed, are mainly based on experiments conducted with small damping values (Weaver & Grover 1978) or neglecting the influence of fluid damping in liquid flows (Tanaka & Takahara 1981)·

The exponent P and the dependence of the stability factor K on the pitch ratio were correlated for different tube configurations and phase state of the cross-flow media· According to a proposition by Chen (1987), the pitch dependence was taken as

$$K(\tau) = a(\tau - b), \tag{8}$$

where a and b are constants· As an example, Figure 1 shows the result for gas flow in a 30° triangular array with the exponent $P = 0{\cdot}5$· The lower bound is equal to the results of Soper (1983)· Although Gross (1975) stated a minimum value of K between $\tau = 1{\cdot}2$ and 1·3 we took K constant for values $\tau \leq 1{\cdot}2$ to be on the safe side· Figure 2 applies to liquid flow with $P = 0{\cdot}15$· The dependence on the pitch ratio is lower, but evident when comparing the results in the same installation (Troidl 1986; Kassera & Strohmeier 1994). The influence of the pitch ratio for all tube configurations can be seen in Tables 2 and 3.

The reference basis for the structural parameters was also varied. So, first the dimensionless mass-damping parameters in liquid flow were calculated with structural data in air, as far as the data were available. In this case, the scatter of the data for all tube configurations and flow regimes was higher, for all exponents P between 0 and 0·5. In other investigations, the pitch velocity was chosen instead of the maximum gap velocity. Although the deviation

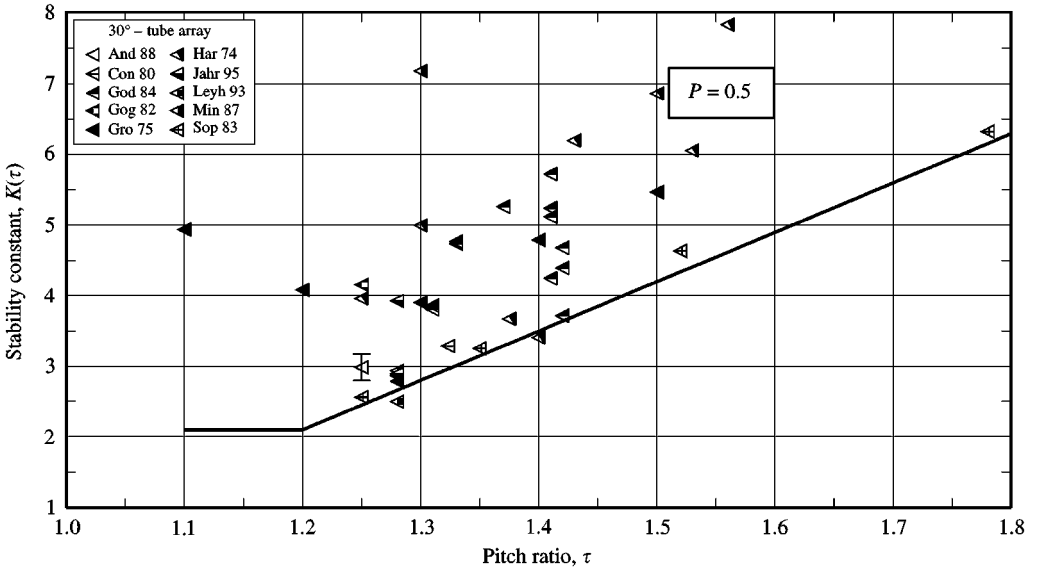

Figure 1. Effect of pitch ratio on the stability constant for gas flow and 30° tube arrays. The contractions in the legend as rather obvious and will not be elaborated; e.g. 'And 88' stands for Andjelić (1988), 'Con 80' for Connors (1980), and so on.

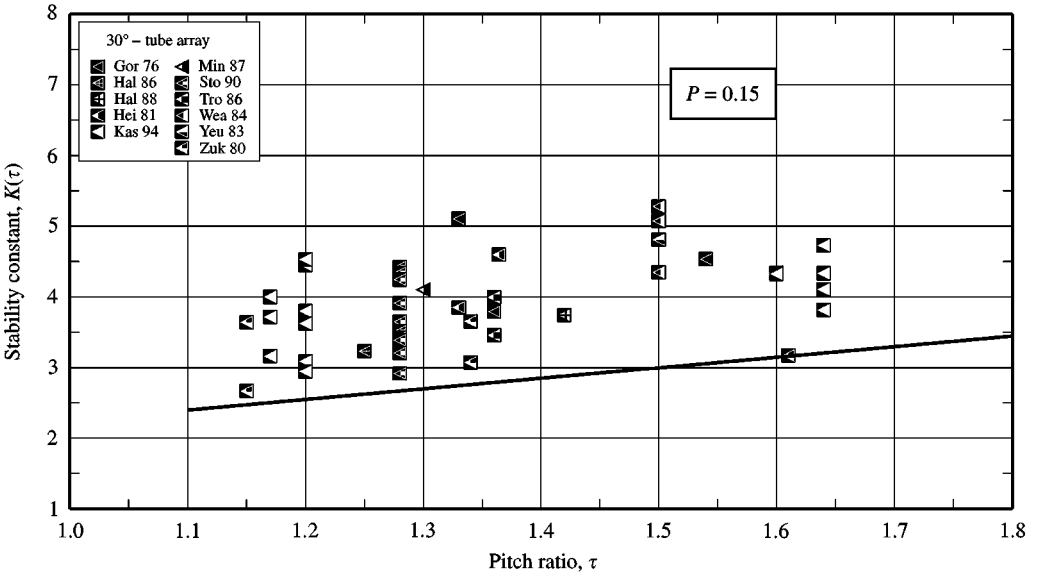

Figure 2. Effect of pitch ratio on the stability constant for liquid flow and 30° tube arrays.

TABLE 2

Stability constants and exponents for standard tube arrays and gas flow

Configuration	K_{min}	$f(\tau) \geq 1$	$K(\tau)$	P	Δ
Tube row (Chen 1987)	4·4	1·36 ($\tau - 0{\cdot}375$)	6·0 ($\tau - 0{\cdot}375$)	0·5	3–300
30°	2·1	3·33 ($\tau - 0{\cdot}9$)	7·0 ($\tau - 0{\cdot}9$)	0·5	2–4000
45°	2·1	2·52 ($\tau - 0{\cdot}8$)	5·3 ($\tau - 0{\cdot}8$)	0·5	2–300
60°	3·1	1	3·1	0·4	2–200
90°	4·1	0·7 τ	2·9 τ	0·4	2–200

TABLE 3

Stability constants and exponents for standard tube arrays and liquid flow

Configuration	K_{min}	$f(\tau) \geq 1$	$K(\tau)$	P	Δ
Tube row (Chen 1982)	2·2	1·41 ($\tau - 0{\cdot}375$)	3·1 ($\tau - 0{\cdot}375$)	0·15	0·05–3
30°	2·4	0·625 ($\tau + 0{\cdot}5$)	1·5 ($\tau + 0{\cdot}5$)	0·15	0·05–2
45°	2·2	0·55 ($\tau + 0{\cdot}6$)	1·2 ($\tau + 0{\cdot}6$)	0·15	0·05–2
60°	1·9	1	1·9	0·15	0·05–2
90°	1·9	0·53 ($\tau + 0{\cdot}7$)	1·0 ($\tau + 0{\cdot}7$)	0·15	0·05–2

of the data is nearly the same for both definitions, it is more advantageous to use the maximum gap velocity, because the results for staggered and in-line arrays can be presented in part together in one stability map each.

6. DESIGN GUIDELINES

The stability equation is found to be

$$u_k^* = \frac{u_{sk}}{f_1 d_a} = K(\tau)\,\Delta^P = K_{\min}\, f(\tau) \left[\frac{m\Lambda}{\rho d_a^2}\right]^P, \tag{9}$$

with $K_{\min}$ bring the lowest K-factor, and $f(\tau)$ is a function of the pitch ratio, ≥ 1. The exponent P is different for gas and liquid flow and depends partly on the tube array. The equations to calculate the stability constants are listed in Table 2 for gas flow and in Table 3 for liquid flow.

A condensed presentation of the influence of pitch ratio on the stability constant can be seen from Figures 3 and 4. The lowest values for the stability constant can be observed for the 60° tube configuration in liquid flow. Due to the alternating in-line flow for this tube configuration, the damping-controlled excitation mechanism is dominant, and the stability constant is therefore independent of the pitch ratio (Chen 1987). The stability constants for normal square arrays (90°) are higher, and a slight influence on the pitch ratio can be observed in liquid and gas flow. The staggered tube configurations (45 and 30°) show a stronger dependence on the pitch ratio because the stiffness-controlled excitation is dominant at the stability point. The strongest influence of the pitch ratio and the highest values for the stability constants can be determined for the tube row.

All experimental data are presented in the stability map for the normal triangular array (30°) and the rotated square array (45°) in Figure 5, and for the rotated triangular array (60°) and the normal square array (90°) in Figure 6. The lines representing the suggested correlations and the experimental data are calculated for a pitch ratio of $\tau = 1{\cdot}20$. The exponent P for gas flow was found to be 0·5 for the 30°- and 45°-configuration, and 0·4 for the 60°- and 90°-tube arrays. Weaver & Fitzpatrick (1988) recommend a slope of 0·3 for the

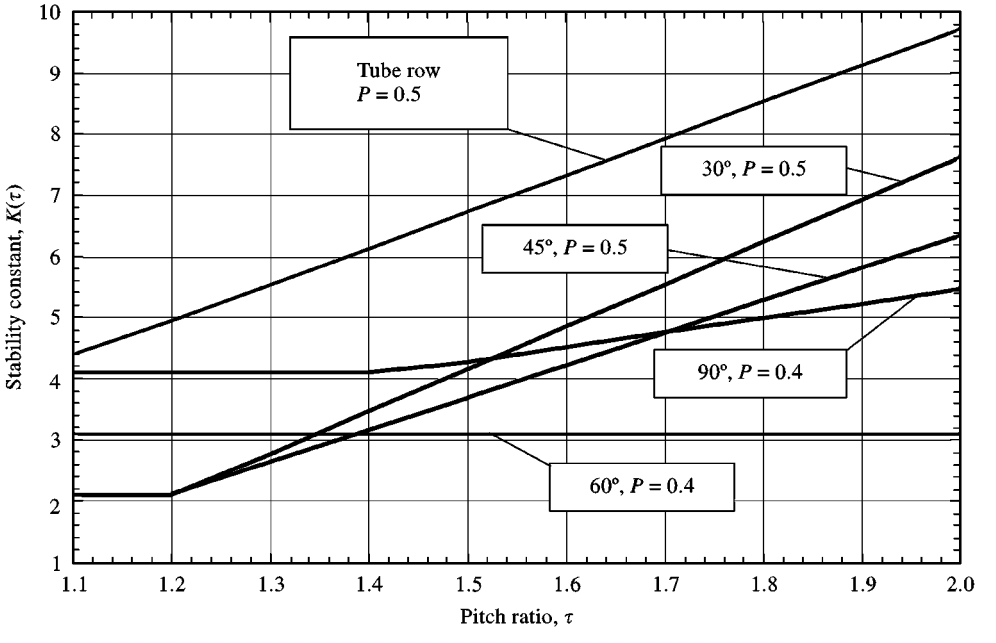

Figure 3. Dependence of stability constants on the pitch ratio for standard tube arrays and gas flow.

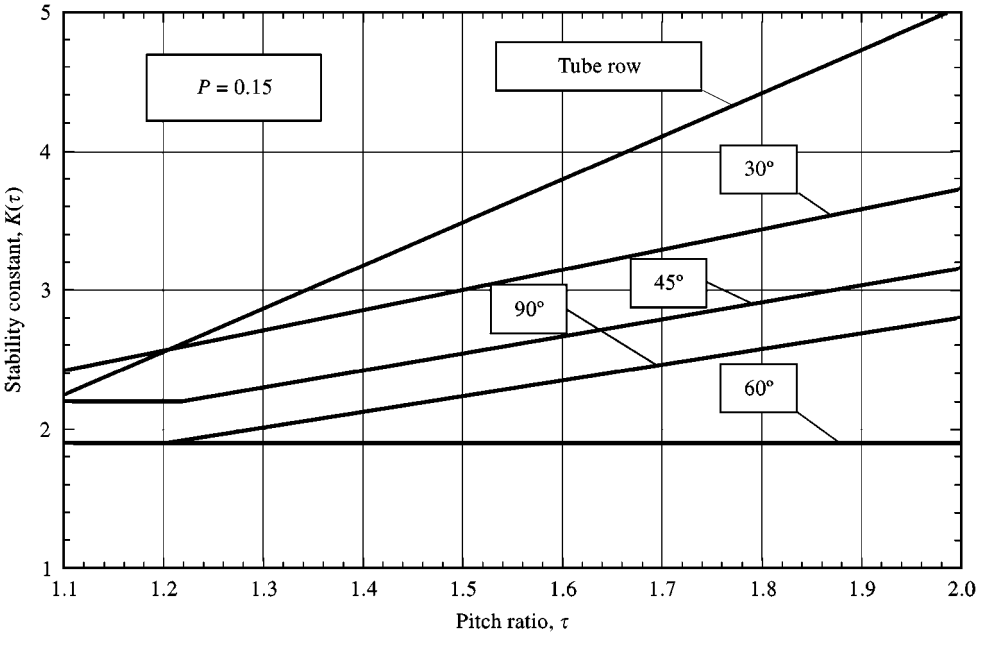

Figure 4. Dependence of stability constants on the pitch ratio for standard tube arrays and liquid flow.

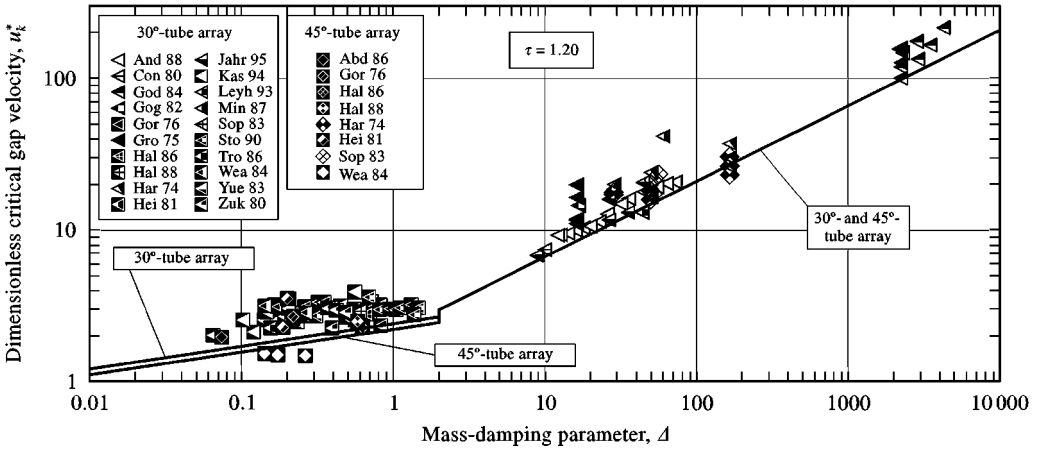

Figure 5. Stability map of dimensionless critical flow velocity versus mass-damping parameter for 30°- and 45°-tube arrays with $\tau = 1{\cdot}20$. Refer to caption of Figure. 1 for meaning of contractions in the legend.

60°-tube array, based on the results of Weaver & Grover (1978) at very low mass-damping parameters. The results of Austermann (1993) show in the technically relevant region of the mass-damping parameter ($\Delta = 10-90$) a slope between 0·33 and 0·40. Theory (Price 1995) indicates a slope of 0·5 in the region $\Delta > 200$. We took a mean value of 0·4. The optimal exponents P for liquid flow were found to vary between 0·10 and 0·25, which was of the same order of magnitudes predicted by Chen (1987). The choice of the mean value 0·15 does not lead to sensibly larger deviations.

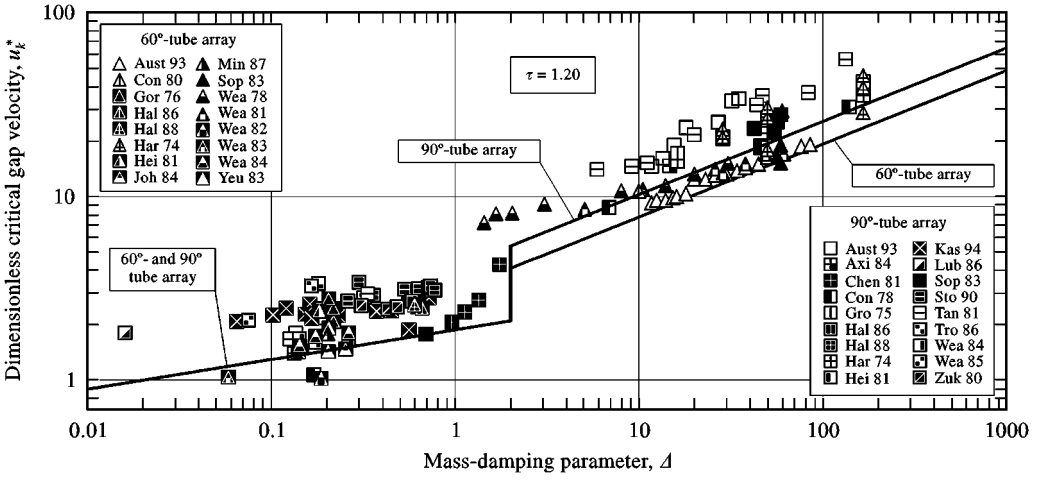

Figure 6. Stability map of dimensionless critical flow velocity versus mass-damping parameter for 60°- and 90°-tube arrays with $\tau = 1{\cdot}20$.

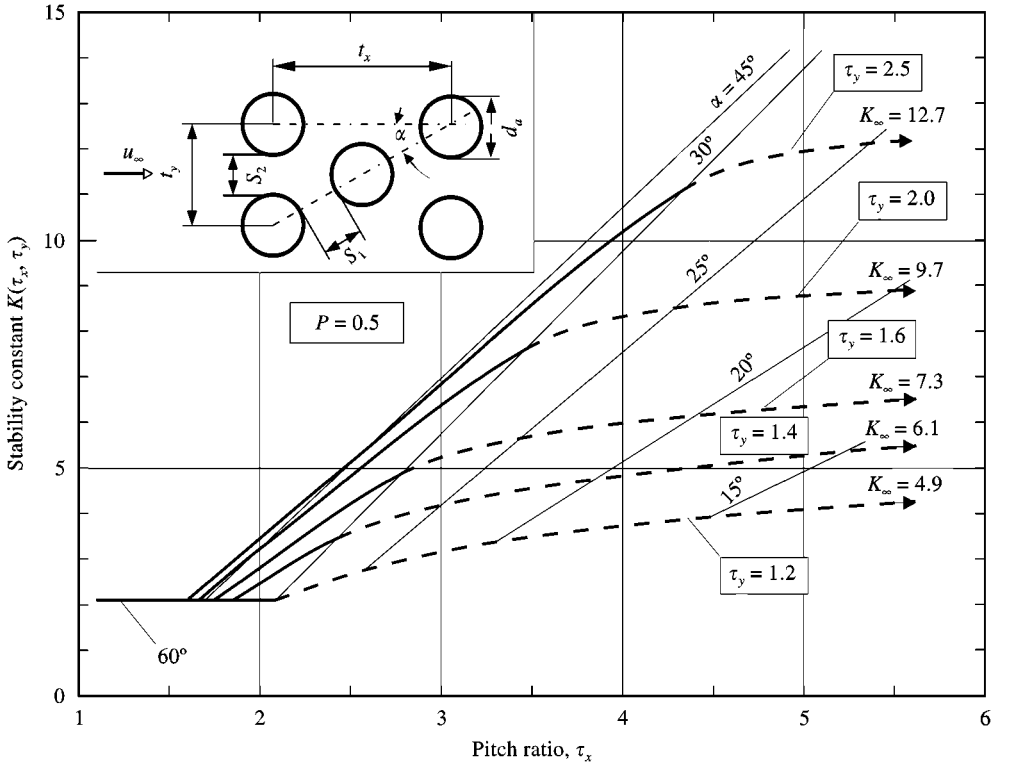

Figure 7. Stability constants for gas flow and non-standard staggered tube arrays.

A reasonable interpolation for non-standard staggered configurations can be obtained from the significant gradation of the stability constants as a function of the pitch ratio and the tube bundle configuration, as illustrated in Figure 7 for gas flow. The stability constant for uniform values of the pitch ratio in the lift direction, τ_y, is presented versus the pitch ratio

TABLE 4

Quantitative comparison with existing guidelines

Tube configuration	Guideline	R.m.s. error [%]	Data below guideline (<4%)	
			Number	Max. deviation [%]
30° gas flow. 63 data points	Present work	26·3	1	6·2
	ASME Code (1992)	38	0	0
	Blevins (1984)	39·1	0	0
	Chen (1987)	30·8	0	0
	Païdoussis (1981)	45·6	0	0
	Pettigrew & Taylor (1991)	27·5	9	19·9
	Weaver & Fitzpatrick (1988)	46·1	0	0
30° liquid flow. 55 data points (27 data points)*)	Present work	28·3/(31·1)*	0/(0)*	0·0/(0·0)*
	ASME Code (1992)	55·2/(56·0)*	0/(0)*	0·0/(0·0)*
	Blevins (1984)	39·8/(33·4)*	0/(0)*	0·0/(0·0)*
	Chen (1987)*)	56·7/(40·2)*	0/(0)*	0·0/(0·0)*
	Païdoussis (1981)	36·5/(45·9)*	5/(2)*	38·5/(13·8)*
	Pettigrew & Taylor (1991)	46·0/(59·3)*	2/(2)*	14·8/(14·8)*
	Weaver & Fitzpatrick (1988)*)	31·4/(32·9)*	2/(0)*	18·6/(0·0)*
45° gas flow. 13 data points	Present work	24·7	1***)	16·8
	ASME Code (1992)	57·6	0	0
	Blevins (1984)	58·4	0	0
	Chen (1987)	43·9	0	0
	Païdoussis (1981)	57	0	0
	Pettigrew & Taylor (1991)	48	0	0
	Weaver & Fitzpatrick (1988)	38·2	0	2·7
45° liquid flow. 6 data points**) (3 data points)*)	Present work	30·1/(49·4)*	0/(0)*	0·0/(0·0)*
	ASME Code (1992)	67·7/(88·2)*	0/(0)*	0·0/(0·0)*
	Blevins (1984)	50·7/(68·0)*	0/(0)*	0·0/(0·0)*
	Chen (1987)*)	59·3/(89·2)*	0/(0)*	0·0/(0·0)*
	Païdoussis (1981)	47·8/(81·4)*	0/(0)*	0·0/(0·0)*
	Pettigrew & Taylor (1991)	60·4/(89·3)*	0/(0)*	0·0/(0·0)*
	Weaver & Fitzpatrick (1988)*)	37·7/(38·7)*	0/(0)*	0·0/(0·0)*
60° gas flow. 48 data points	Present work	27·4	0	3·4
	ASME Code (1992)	32·3	1	4·2
	Blevins (1984)	33·4	0	2
	Chen (1987)	25·9	10	21·6
	Païdoussis (1981)	28·5	2	35·9
	Pettigrew & Taylor (1991)	24·5	17	30·3
	Weaver & Fitzpatrick (1988)	28·7	0	0
60° liquid flow. 13 data points**) (8 data points)*)	Present work	26·4/(32·0)*	0/(0)*	3·9/(3·9)*
	ASME Code (1992)	48·9/(69·5)*	0/(0)*	0·0/(0·0)*
	Blevins (1984)	22·8/(34·0)*	2/(2)*	16·4/(16·4)*
	Chen (1987)*)	18·6/(26·8)*	4/(1)*	29·0/(45·6)*
	Païdoussis (1981)	24·4/(53·3)*	4/(4)*	37·8/(37·8)*
	Pettigrew & Taylor (1991)	37·3/(72·0)*	0/(0)*	0·0/(0·0)*
	Weaver & Fitzpatrick (1988)*)	53·1/(42·6)*	2/(0)*	48·2/(0·0)*

TABLE 4. *Continued*

	Present work	29·3	0	1·8
	ASME Code (1992)	41·9	0	0
90° gas flow.	Blevins (1984)	43·1	0	0
39 data points	Chen (1987)	46·6	0	0
	Païdoussis (1981)	42·1	0	2·7
	Pettigrew & Taylor (1991)	29·6	3	14·7
	Weaver & Fitzpatrick (1988)	43·4	0	0
	Present work	36·2/(30·1)*	1/(0)****)	35·7/(0·0)*
	ASME Code (1992)	50·4/(59·7)*	0/(0)*	0·0/(0·0)*
90° liquid flow.	Blevins (1984)	31·0/(31·2)*	5/(1)*	55·1/(10·7)*
50 data points	Chen (1987)*)	34·6/(30·1)*	3/(5)*	34·2/(26·1)*
(25 data points)*)	Païdoussis (1981)	34·5/(47·1)*	13/(3)*	69·0/(23·9)*
	Pettigrew & Taylor (1991)	39·9/(62·8)*	5/(0)*	20·9/(0·0)*
	Weaver & Fitzpatrick (1988)*)	38·5/(22·5)*	1/(0)*	16·7/(0·0)*

Remarks

*) For the calculated values in brackets the structural parameters were used as in each guideline recommended. So, for the values calculated with the equations given by Chen (1987) the structural parameters were used in still air even for the liquid region. The values for the guideline of Weaver & Fitzpatrick (1988) were calculated with the damping determined in still air. The structural data in air are available for nearly the half of all considered data.
All data presented without brackets were calculated with structural parameters determined in still fluid.
**) Three data points from Weaver & Yeung (1984) for the 45° tube array and two data for a 60° tube array by Weaver & Koroyannakis (1982) and Weaver & Koroyannakis (1983) were not considered; the fluidelastic instability in those cases was influenced by resonant vortex excitation.
***) Hartlen (1974), see Section 7.
****) Connors (1978), see Section 7.

TABLE 5

Present criterion compared with previously available ones, for cases of similar performance (in terms of r.m.s. error)

	Present criterion r.m.s. error (%)		Best of existing criteria r.m.s.-error (%)
30° gas flow	26	Chen (1987)	31
30° liquid flow	28 (31)	Weaver & Fitzpatrick (1988)	31 (33)
45° liquid flow	30 (49)	Weaver & Fitzpatrick (1988)	38 (39)
60° gas flow	27	Weaver & Fitzpatrick (1988)	29
90° liquid flow	36 (30)	Weaver & Fitzpatrick (1988)	39 (23)

in the drag direction, τ_x. Stability constants for tube rows are limiting values for infinite pitch ratio in the drag direction. The exponent of the mass damping parameter is $P = 0{\cdot}5$ for the three standard configuration angles α. A similar diagram was derived for staggered tube arrays and liquid flow.

7. DISCUSSION

The object of this investigation was to find a guideline for the standard tube configurations on the lower bound, but without any unnecessary safety factor. Therefore, some

experimental data near or below the lower bound in Figures 5 and 6 will be discussed. In liquid flow, three data points by Weaver & Yeung (1984) determined in a 45°- tube array and two data points by Weaver & Koroyannakis (1982, 1983) determined in a 60°-configuration were ignored. We have included these points in Figures 5 and 6 as a warning to industrial users, in order to keep in mind the negative influence of vortex excitation on fluidelastic instability. In these experiments, with very low damping values, resonant vortex excitation occurred at a velocity which was about 20% lower than the expected instability value. Due to this "external" force and the resulting high resonance amplitude, the unstable limit cycle was reached and fluidelastic instability was stimulated at a lower velocity [see Austermann & Popp (1995)]. An intensification of this effect may be produced by careful frequency tuning of the tubes, which normally will not be found in real heat exchangers.

One data point, also in liquid flow in a 90°-tube array, by Connors (1978) deviates widely from the other 49 data points. Connors measured only one point with water in his investigation, and the structural data for the model are not explicitly presented; therefore, this point was not considered. In gas flow, one data point by Hartlen (1974) for a 45°-tube array has a deviation of 17%. This point, at a mass-damping parameter of 166, shows a diverging tendency in the dependence on the pitch ratio in comparison to the other data of Hartlen and the data by Soper (1983) for this tube array.

Pettigrew & Taylor (1991) recommend an exponent of 0·5 for the mass-damping parameter for liquid and gas flow. It can be seen from Figures 5 and 6, that this assumption does not agree with the slope of the experimental data [e.g., Kassera & Strohmeier (1994) and Stockmeier (1990)] and leads to a strong deviation in the case of low mass-damping parameters. The experimental data by Chen & Jendrzejczyk (1981) for a 90°-tube array represent very well the transitional limit between liquid and gas flow at about $\Delta = 2$ in Figure 6.

Two-phase flow was not considered in the correlations presented, because an analysis of the most recent experimental data shows that, at present, there is a lack of understanding of the phenomena occurring, and no basis exists for a generally valid description of the vibrations induced by two-phase flow.

8. COMPARISON WITH EXISTING GUIDELINES

The following guidelines for estimating the fluidelastic instability in uniform single-phase cross-flow were compared with our new proposal: ASME Code (1992), Blevins (1984), Chen (1987), Païdoussis (1981), Pettigrew & Taylor (1991) and Weaver & Fitzpatrick (1988). The relative root-mean-square error (r.m.s.) is computed by equation (5) as recommended by Blevins (1984). For every guideline, the basis of the calculation is the square of the difference between a measured and the corresponding predicted value, related to the measured value, for all data points N. Table 4 shows the results for all tube arrays separated for gas and liquid flow. The dimensionless critical velocity and the mass-damping parameter are at first, when considering all the data, calculated with the structural parameters in still fluid, also for the guideline by Chen (1987), who suggested to take them always in air, and Weaver & Fitzpatrick (1988), who recommend to take the damping in air. Secondly, when considering only nearly half of the liquid data, for which the structural data in air are known, the dimensionless critical velocity and the mass-damping parameter were calculated as recommended in each of the guidelines. The relative r.m.s. error values determined in this way are plotted in brackets. Table 4 shows that the new design equations are always on the safe side (excluding two data points discussed in Section 7) and are in five

TABLE 6

Present criterion compared with previously available ones, for cases where the present criterion performance is superior

	Present criterion r.m.s. error (%)		Best of existing criteria r.m.s.-error (%)
45° gas flow	25	Weaver & Fitzpatrick (1988)	38.2
60° liquid flow	26 (32)	Weaver & Fitzpatrick (1988)	53 (43)
		Pettigrew & Taylor (1991)	37 (72)
90° gas flow	29	Weaver & Fitzpatrick (1988)	43
		Païdoussis (1981)	42
		Blevins (1984)	43

cases comparable with the best existing guidelines, concerning the r.m.s.-error value, as shown in Table 5.

In three cases, the new correlations are substantially better than the existing guidelines, as shown in Table 6.

This comparison demonstrates that the best existing guidelines are in one case that of Chen (1987) and in all other cases those of Weaver & Fitzpatrick (1988). In Figure 8 the new design recommendations are plotted together with five of the six evaluated existing guidelines in stability maps for the standard tube configurations at $\tau = 1{\cdot}2$, for the 30°- and 45°- tube array also at $\tau = 2{\cdot}0$. The problem comparing the guidelines for liquid flow with those given by Chen (1987) and Weaver & Fitzpatrick (1988) can be seen in Figure 8 for the 30°- tube array. Additional threshold lines are plotted for the liquid region, which is assumed to begin at values Δ lower than 2·0, with estimated mass and damping values in liquid being two times those in gas. In these cases, the frequency for still fluid was recalculated with equation (3) to determine the dimensionless critical velocity.

9. CONCLUSIONS

A comparison of six existing guidelines for estimating the fluidelastic instability threshold in uniform single-phase cross-flow led to new design recommendations, which are in five cases comparable with the identified best guidelines and in three cases substantially better. The exponents of the mass-damping parameter were found to be in gas flow 0·5 for the 30°- and 45°- configuration, 0·4 for the 60°- and 90°- configuration, and in liquid flow 0·15 for all tube arrays. The stability constants are, except for the 60°-tube array, functions of the pitch ratio with a significant gradation, which enables a reasonable interpolation for non-standard configurations. All structural parameters are to be determined in still fluid.

The new recommendations provide an improved basis for the practical design of real tube-bundle heat exchangers. All further aspects, e.g. considering flow distribution, inclined flow, vortex shedding, acoustic resonance and turbulent buffeting are not the subject of this paper, but are dealt with elsewhere (Gelbe *et al.* 1997).

ACKNOWLEDGEMENT

The AIF-project No. 10608N was promoted by the fund of the German minister of economics.

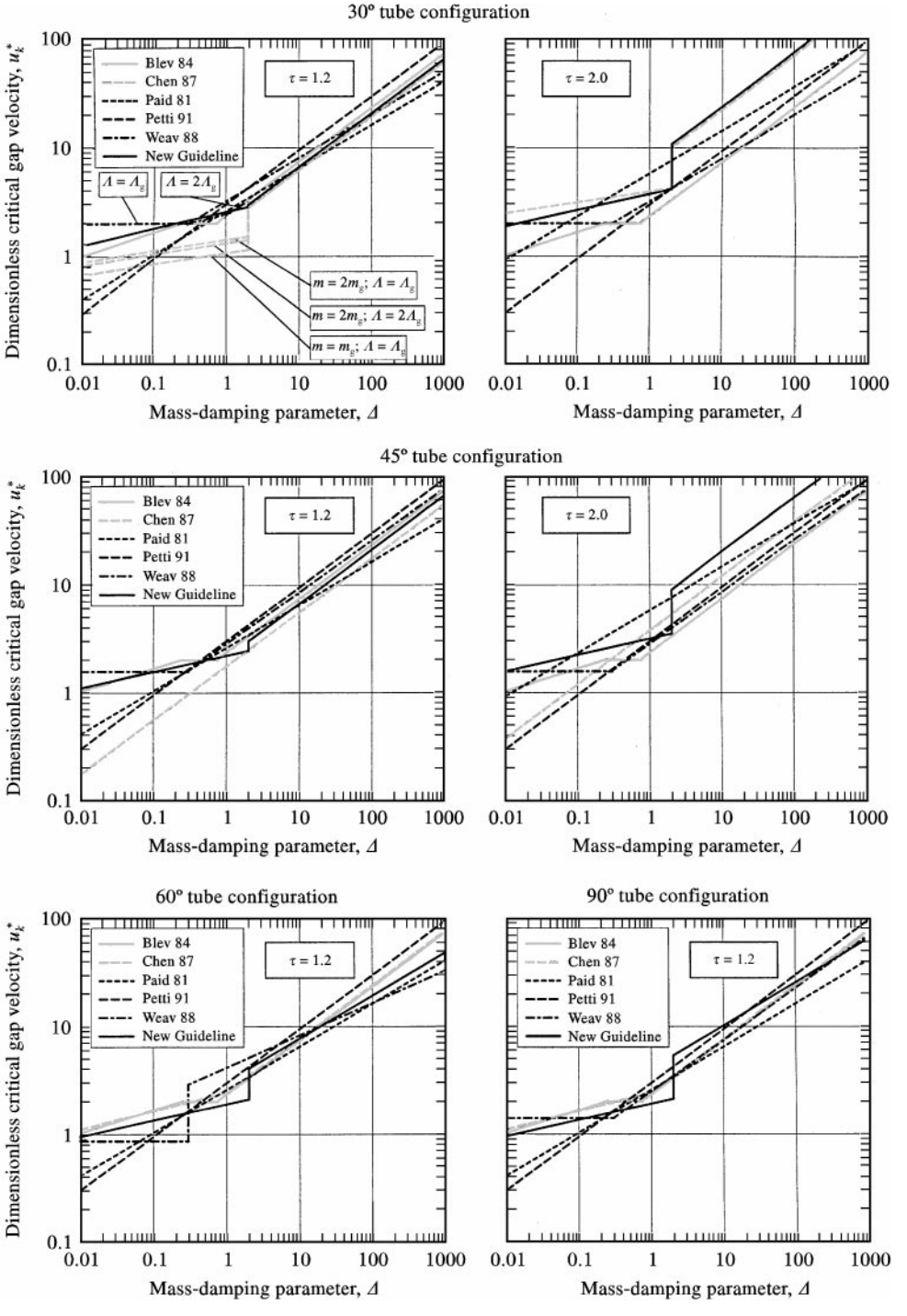

Figure 8. Comparison of design recommendations. Dimensionless critical flow velocity as a function of the mass-damping parameter.

References

Abd-Rabbo, A. & Weaver, D. S. 1986 A flow visualization study of flow development in a staggered tube array. *Journal of Sound and Vibration* **106,** 241–256.

Andjelić, M. 1988 Stabilitätsverhalten querangeströmter Rohrbündel mit versetzter Dreiecksteilung. Dissertation, Universität Hannover.

Andjelić, M. & Popp, K. 1989 Stability effects in a normal triangular cylinder array. *Journal of Fluids and Structures* **3,** 165–185.

ASME Pressure Vessel Code, Section III, Division 1 1992 Flow-induced vibration of tubes and tube banks. *Nonmandatory Appendix*, Appendix N-1300, pp. 364–381.

Austermann, R. 1993 Zum Schwingungsverhalten querangeströmter Rohrbündel bei Anregung vom Galloping-Typ. Dissertation, Universität Hannover.

Austermann, R. & Popp, K. 1995 Stability behaviour of a single flexible cylinder in rigid tube arrays of different geometry subjected to cross-flow. *Journal of Fluids and Structures* **9,** 303–322.

Axisa, F., Villard, B., Gibert, R. J., Hetsroni, G. & Sundheimer, P. 1984 Vibration of tube bundles subjected to air–water and steam–water cross flow: preliminary results on fluidelastic instability. (eds M. P. Païdoussis, M. K. Au-Yang & S. S. Chen), *Proceedings of ASME Symposium on Flow-Induced Vibrations* New Orleans, **2,** pp. 269–284. New York: ASME.

Blevins, R. D., Gibert, R. J. & Villard, B. 1981 Experiments on vibration of heat exchanger tube arrays in cross flow. *Transactions of 6th International Conference on Structural Mechanics in Reactor Technology* (*SMIRT*), Paper B6-9.

Blevins, R. D. 1984 Discussion of guidelines for instability flow velocity of tube arrays in crossflow. *Journal of Sound and Vibration* **97,** 641–644.

Chen, S. S. & Jendrzejczyk, J. A. 1981 Experiments on fluid instability in tube banks subjected to liquid cross flow. *Journal of Sound and Vibration* **78,** 355–381.

Chen, S. S. & Jendrzejczek, J. A. 1982 Stability of tube arrays in crossflow. *Nuclear Engineering and Design* **75,** 351–373.

Chen, S. S. 1984 Guidelines for instability flow velocity of tube arrays in crossflow. *Journal of Sound and Vibration* **93,** 439–455.

Chen, S. S. 1987 *Flow-Induced Vibration of Circular Cylindrical Structures.* Washington, DC: Hemisphere Publishing Corporation.

Connors, H. J. 1970 An experimental investigation of the flow-induced vibration of tube arrays in cross flow. Ph.D. Thesis, University of Pittsburgh.

Connors, H. J. 1978 Fluidelastic vibration of heat exchanger tube arrays. *ASME Journal of Mechanical Design* **100,** 347–353.

Connors, H. J. 1980 Fluidelastic vibration of tube arrays excited by nonuniform cross flow. In *Flow-Induced Vibration of Power Plant Components*, Publication PVP-Vol. 41, pp. 93–107.

Eisinger, F. L. 1980 Prevention and cure of flow-induced vibration problems in tubular heat exchangers. *ASME Journal of Pressure Vessel Technology* **102,** 138–145.

Gelbe, H., Schröder, K. & Ziada, S. 1997 *Schwingungen in Wärmeübertrager-Rohrbündeln* VDI-Wärmeatlas, 8th edition, Chapter Oc, pp. Oc1-Oc33. Berlin: Springer-Verlag.

Gelbe, H., Jahr, M. & Schröder, K. 1995 Flow-induced vibrations in heat exchanger tube bundles. *Chemical Engineering and Processing* **34,** 289–298.

Godon, J. L. 1984 Flows and flow induced vibrations in large condensers. *Proceedings ASME Symposium on Flow-Induced Vibrations* Vibrations in Heat Exchangers (eds M. P. Païdousons, J. M. Chenoweth & M. D. Bernstein) New Orleans, Vol. 3; pp. 1–16. New York: ASME.

Gog, W. 1982 Untersuchungen der Erregermechanismen am Einzelrohr und am querangeströmten Rohrbündel. Dissertation, Technische Universität Berlin.

Gorman, D. J. & Mirza, S. 1976 Experimental development of design criterion to limit liquid flow induced vibration in nuclear reactor steam generators. *Journal of Nuclear Science and Engineering* **61,** 324–336.

Gross, H. 1975 Untersuchung aeroelastischer Schwingungsmechanismen und deren Berücksichtigung bei der Auslegung von Rohrbündelwärmetauschern. Dissertation, Universität Hannover.

Halle, H., Chenoweth, J. M. & Wambsganss, M. W. 1986 Shellside flow-induced tube vibration in typical heat exchanger configurations: overview of a research program. *Proceedings of ASME-PVP Conference*, Chicago, PVP-Vol. 104, pp. 161–169. New York: ASME.

Halle, H., Chenoweth, J. M. & Wambsganss, M. W. 1988 Shellside waterflow-induced tube vibration in heat exchanger configurations with tube pitch-to-diameter ratio of 1.42. *Proceedings International Symposium on Flow-Induced Vibration and Noise*, Chicago, Vol. 3:

Flow-Induced Vibration in Heat Transfer Equipment (eds M. P. Païdoussis *et al.*), pp. 1–16. New York: ASME.

Hartlen, R. T. 1974 Wind-tunnel determination of fluid-elastic-vibration thresholds for typical heat-exchanger tube patterns. Ontario Hydro Research Devision, Report 74-309-K.

Heilker, W. J. & Vincent, R. Q. 1981 Vibration in nuclear heat exchangers due to liquid and two-phase flow. *ASME Journal of Engineering for Power* **103,** 358–365.

Jahr, M. 1995. Einflüsse von Strukturparametern und Strömungsverteilung auf das Schwingverhalten mit Luft angeströmter Rohrbündel. Dissertation, Technische Universität Berlin (also in: *Flow-Induced Vibration and Wear*, 1994, PVP-Vol. 273, pp. 7–13. New York: ASME).

Johnson, D. K. & Schneider, W. G. 1984 Flow-induced vibration of a tube array with an open lane. *Proceedings of ASME Symposium on Flow-Induced Vibrations*, New Orleans, Vol. 3: Vibration in Heat Exchangers (eds M. P. Païdoussis, J. M. Chenoweth & M. D. Bernstein), pp. 63–72. New York: ASME.

Kassera, V. & Strohmeier, K. 1994 Experimental determination of tube bundle vibrations induced by cross flow. *ASME PVP Conference*, Minneapolis, PVP-Vol. 273, pp. 91–97; (also personal information about detailed experimental data).

Leyh, T. 1993 Strömungsinduzierte Rohrbündelschwingungen in einem gasdurchströmten realen Wärmeübertrager. Dissertation, Technische Universität Berlin.

Lubin, B. T., Letendre, R. P., Quinn, J. W. & Kenny, R. A. 1986 Comparison of the response of a scale model and prototype design tube bank structure to cross-flow induced fluid excitation. *ASME PVP Conference*, Chicago, PVP-Vol. 104, pp. 171–177.

Minakami, K. & Ohtomi, K. 1987 Flow direction and fluid density effects on the fluidelastic vibrations of a triangular array of tubes. *International Conference on Flow Induced Vibrations*, Bowness-on-Windermere, Paper B2, pp. 65–75.

Païdoussis, M. P. 1981 Fluidelastic vibration of cylinder arrays in axial and cross flow — A review of the state of the art, *Flow-Induced Vibration Design Guidelines* (ed. P. Y. Chen), pp. 11–46, New York: ASME.

Pettigrew, M. J., Goyder, H. G. D., Qiao, L. Z. & Axisa, F. 1986a Damping of multispan heat exchanger tubes, Part I: in gases. *ASME PVP Conference*, Chicago, Vol. 104, pp. 81–87.

Pettigrew, M. J., Rogers, R. J. & Axisa, F. 1986b Damping of multispan heat exchanger tubes, Part II: in liquids. *ASME PVP Conference*, Chicago, Vol. 104, pp. 89–98.

Pettigrew, M. J. & Taylor, C. E. 1991 Fluid-elastic instability of heat exchanger tube bundles: review and design recommendations. *International Conference on Flow-Induced Vibration*, Brighton, Paper C 416/015, *Proceedings of Institution of Mechanical Engineers*, pp. 349–368.

Price, S. J. 1995 A review of theoretical models for fluidelastic instability of cylinder arrays in cross-flow. *Journal of Fluids and Structures*, **9,** 463–518.

Scott, P. M. 1987. Flow visualization of cross-flow induced vibration in tube arrays. M. Eng. Thesis, McMaster University, Hamilton, Ontario, Canada.

Soper, B. M. H. 1983. The effect of tube layout on the fluid-elastic instability of tube bundles in cross flow. *ASME Journal of Heat Transfer* **105,** 744–750.

Stockmeier, D. 1990 Einfluß der Viskosität auf die Schwingungen in Rohrbündelapparaten, Dissertation, Universität Hannover.

Tanaka, H. & Takahara, S. 1981. Fluidelastic vibration of a tube array in cross-flow. *Journal of Sound and Vibration* **77,** 19–37.

Troidl, H. 1986. Strömungsinduzierte Schwingungen querangeströmter Rohrbündel bei versetzter und fluchtender Rohranordnung, Dissertation, Technische Universität München.

Weaver, D. S. & Grover, L. K. 1978 Cross-flow induced vibrations in a tube bank — turbulent buffeting and fluid elastic instability. *Journal of Sound and Vibration* **59,** 277–294.

Weaver, D. S. & El-Kashlan, M. 1981 The effect of damping and mass ratio on the stability of a tube bank. *Journal of Sound and Vibration* **76,** 283–294.

Weaver, D. S. & Koroyannakis, D. 1982 The cross-flow response of a tube array in water — a comparison with the same array in air. *ASME Journal of Pressure Vessel Technology* **104,** 139–146.

Weaver, D. S. & Koroyannakis, D. 1983 Flow-induced vibrations of heat exchanger U-tubes: a simulation to study the effects of asymmetric stiffness. *ASME Journal of Vibration, Acoustics, Stress and Reliability in Design* **105,** 67–75.

Weaver, D. S. & Yeung, H. C. 1984 The effect of tube mass on the flow induced response of various tube arrays in water. *Journal of Sound and Vibration* **93,** 409–425.

WEAVER, D. S. & ABD-RABBO, A. 1985. A flow visualization study of a square array of tubes in water cross-flow. *ASME Journal of Fluids Engineering* **107,** 354–363.
WEAVER, D. S. & FITZPATRICK, J. A. 1987 A review of flow-induced vibration in heat-exchangers. In *Proceedings International Conference Flow-Induced Vibration*, Bowness-on-Windermere, Paper A1, pp. 1–17.
WEAVER, D. S. & FITZPATRICK, J. A. 1988 A review of flow-induced vibration in heat-exchangers. *Journal of Fluids and Structures* **2,** 73–93.
YEUNG, H. C. & WEAVER, D. C. 1983. The effect of approach flow direction on the flow induced vibrations of a triangular tube array. *ASME Journal of Mechanical Design* **105,** 76–82.
ŽUKAUSKAS, A. & KATINAS, V. 1980. Flow-induced vibrations in heat-exchanger tube banks. IUTAM Symposium Karlsruhe 1979. In *Practical Experiences with Flow-Induced Vibrations* (eds E. Naudascher & D. Rockwell). Berlin: Springer.

APPENDIX: NOMENCLATURE

c_h	dimensionless hydrodynamic mass coefficient
d_a	tube diameter (m)
f_i	tube natural frequency of mode i (Hz)
K	stability constant
L	tube length (m)
m	total mass per unit length (kg/m)
m_h	hydrodynamic mass per unit length (kg/m)
N	number of span lengths
P	exponent of mass-damping parameter
s	wall thickness of tube (m)
t	pitch (m)
u_∞	upstream velocity (m/s)
u^*	dimensionless gap velocity
u_s	maximum gap velocity (m/s)
α	configuration angle for staggered tube arrays (deg)
Δ	mass-damping parameter
ζ	damping ratio
Λ	logarithmic decrement of damping
ρ	shell side fluid density (kg/m^3)
τ	pitch ratio

Subscripts

a	outer side of tube
f	fluid
g	gas phase
k	critical point
l	liquid phase
s	gap between two tubes
x	drag direction
y	lift direction
τ	bundle